original reports

Functional Engagement of the PD-1/PD-L1 Complex But Not PD-L1 Expression Is Highly Predictive of Patient Response to Immunotherapy in Non–Small-Cell Lung Cancer

Lissete Sánchez-Magraner, PhD[1]; Juan Gumuzio, PhD[1]; James Miles, PhD[1]; Nicole Quimi, MSc[1]; Purificación Martínez del Prado, MD[2]; María Teresa Abad-Villar, MD[2]; Fernando Pikabea, MD[2]; Laura Ortega, MD[2]; Carmen Etxezarraga, MD[2]; Salvador Martín-Algarra, MD[3]; María D. Lozano, MD[3]; Mónica Saiz-Camin, MD[4]; Mikel Egurrola-Izquierdo, MD[5]; Inmaculada Barredo-Santamaría, MD[5]; Alberto Saiz-López, MD[5]; Jenifer Gomez-Mediavilla, MD[6]; Nerea Segues-Merino, MD[6]; María Aranzazu Juaristi-Abaunz, MD[6]; Ander Urruticoechea, MD[6]; Erica J. Geraedts, MD[7]; Kim van Elst, MD[7]; Niels J.M. Claessens, MD[8]; Antoine Italiano, MD[9]; Christopher J. Applebee, MSc[1]; Sandra del Castillo, BSc[1,10]; Charles Evans, MSc[1]; Fernando Aguirre, MSc[1]; Peter J. Parker, PhD[1,11,12]; and Véronique Calleja, PhD[1]

abstract

PURPOSE In many cancers, the expression of immunomodulatory ligands leads to immunoevasion, as exemplified by the interaction of PD-L1 with PD-1 on tumor-infiltrating lymphocytes. Profound advances in cancer treatments have come with the advent of immunotherapies directed at blocking these immuno-suppressive ligand-receptor interactions. However, although there has been success in the use of these immune checkpoint interventions, correct patient stratification for these therapies has been challenging.

MATERIALS AND METHODS To address this issue of patient stratification, we have quantified the intercellular PD-1/PD-L1 interaction in formalin-fixed paraffin-embedded tumor samples from patients with non–small cell lung carcinoma, using a high-throughput automated quantitative imaging platform (quantitative functional proteomics [QF-Pro]).

RESULTS The multisite blinded analysis across a cohort of 188 immune checkpoint inhibitor-treated patients demonstrated the intra- and intertumoral heterogeneity of PD-1/PD-L1 immune checkpoint engagement and notably showed no correlation between the extent of PD-1/PD-L1 interaction and PD-L1 expression. Importantly, PD-L1 expression scores used clinically to stratify patients correlated poorly with overall survival; by contrast, patients showing a high PD-1/PD-L1 interaction had significantly better responses to anti–PD-1/PD-L1 treatments, as evidenced by increased overall survival. This relationship was particularly strong in the setting of first-line treatments.

CONCLUSION The functional readout of PD-1/PD-L1 interaction as a predictive biomarker for the stratification of patients with non–small-cell lung carcinoma, combined with PD-L1 expression, should significantly improve the response rates to immunotherapy. This would both capture patients excluded from checkpoint immunotherapy (high PD-1/PD-L1 interaction but low PD-L1 expression, 24% of patients) and additionally avoid treating patients who despite their high PD-L1 expression do not respond and suffer from side effects.

J Clin Oncol OO. © 2023 by American Society of Clinical Oncology

INTRODUCTION

Immunotherapies against non–small-cell lung carcinoma (NSCLC) have gained traction in recent years,[1] leading to significant improvements in patient outcomes. One of the most targeted immune checkpoints is the PD-1/PD-L1 pathway. Blockade of this checkpoint pathway with the inhibitors currently licensed against PD-1 (nivolumab, pembrolizumab, and cemiplimab) or PD-L1 (atezolizumab and durvalumab) has emerged as a new pillar in cancer treatment. Nevertheless, despite much enthusiasm surrounding the success of these inhibitory drugs on a subset of patients, notably in advanced disease, a significant number of patients do not benefit from these treatments.

To our knowledge, PD-L1 expression level determined by immunohistochemistry (IHC) was the first clinically validated predictive immuno-oncology (IO) biomarker, which has been translated into clinical practice. The codevelopment of different PD-L1 IHC diagnostics using proprietary antibodies has resulted in different US Food and Drug Administration–approved and CE-IVD–marked

CONTEXT

Key Objective

Currently, 60% of patients with non–small-cell lung carcinoma (NSCLC) do not respond to immune checkpoint inhibitor therapies, and hence, there is a real need of new biomarkers for patient selection. Therefore, we sought to quantify PD-1/PD-L1 interaction states using our quantitative functional proteomics platform to predict patient outcome and response to immunotherapy. We then compared the predictive power of PD-1/PD-L1 interaction state with the currently used gold standard, PD-L1 expression scores (tumor proportion score), in a cohort of 135 patients with NSCLC.

Knowledge Generated

PD-1/PD-L1 engagement was evaluated as a novel predictive biomarker in a cohort of 135 patients with NSCLC. PD-1/PD-L1 interaction state was predictive of patient clinical response to immunotherapy (progression-free survival and overall survival). PD-L1 expression level, the current validated biomarker for treatment with PD-1/PD-L1 checkpoint inhibitors, failed to predict patient response and survival.

Relevance *(T.E. Stinchcombe)*

Novel and better predictive biomarkers of immunotherapy benefit are needed. This study provides preliminary evidence that measurement of PD-1/PD-L1 interaction may be clinically useful. Studies in larger cohorts or prospective studies should be considered.*

*Relevance section written by *JCO* Associate Editor Thomas E. Stinchcombe, MD.

assays. Each is linked to a specific drug and scoring system with its own predictive value and given PD-L1 expression cutoff. The stratification of patients for monotherapy is still currently based on high PD-L1 scores (tumor proportion score [TPS] $\geq$ 50%; European Medicines Agency (EMA) threshold criteria—SP263 Ventana). However, there are a high number of nonresponders (53% at 2 years and 62% at 3 years even for those with PD-L1 TPS $\geq$ 50%)[2] owing to resistance to treatment.[3] In addition, many patients experience serious immune-related adverse events (irAEs). Furthermore, studies showing that patients with NSCLC could experience survival benefits with anti–PD-1/PD-L1 treatments regardless of their PD-L1 expression level[4] has led to the realization that better biomarkers are necessary for improved patient treatment stratification.[2,5,6]

We hypothesize that the level of PD-1/PD-L1 engagement is likely a better predictor of response to anti–PD-1/PD-L1 therapy than PD-L1 TPS, the biomarker currently used in clinical practice. However, unlike typical oncogene mutations and subsequent oncoprotein dysregulation, which can be readily monitored to stratify for interventional purposes, PD-1/PD-L1 exists to act as a homeostatic gatekeeper of the immune system and the activation of this immuno-suppressive effector pathway is more difficult to measure. To address this problem, we have used a quantitative functional approach to directly measure PD-1/PD-L1 engagement, the direct target of immune checkpoint inhibitors (ICIs). To do so, we developed a new antibody-based automated imaging platform (quantitative functional proteomics [QF-Pro]) that can quantify protein post-translational modifications and protein-protein interactions in malignant tissue samples (formalin-fixed paraffin-embedded [FFPE]). This platform is based on amplified

Förster resonance energy transfer (FRET), detected by fluorescence lifetime imaging microscopy (FLIM), that provides quantitative interaction measurements.[7-10] This principle has been used previously for the quantification of PD-1/PD-L1 interactions in solid malignancies, illustrating its possible value and highlighting the heterogeneity of this receptor-ligand engagement.[9] Here, we have applied a distinctive amplified FRET platform that exploits new optics to deliver higher-resolution profiles per patient for better accuracy, faster acquisition, and wider fields of view, addressing the heterogeneity challenges in previously constrained tumor sampling. This platform has been used here to analyze a NSCLC cohort (188 patients) by quantifying PD-1/PD-L1 interaction states.

In this study, the retrospective analysis of a cohort of patients with NSCLC demonstrated no correlation between PD-1/PD-L1 functional interaction and PD-L1 expression. PD-L1 expression scores (TPS $\geq$ 50%), which are used to stratify the patients clinically, poorly correlated with patients' overall survival (OS) and progression-free survival (PFS). However, patients showing a high PD-1/PD-L1 interaction had significantly better responses to anti–PD-1/PD-L1 treatments, demonstrated by improved OS and PFS. Remarkably, a subset of patients with a low PD-L1 score experienced an increased response to anti–PD-1/PD-L1 treatments, but only if they displayed strong receptor-ligand interactions (ie, a high FRET efficiency).

MATERIALS AND METHODS

Antibodies and Reagents

See the Data Supplement (online only; Appendix I) for a detailed list of antibodies and reagents.

NSCLC Cohort

Biopsies from NSCLC tumors were obtained during interventional radiology procedures or surgery, and all patients provided written informed consent. See the Data Supplement [Appendix I] for details regarding the origin of patient samples and Science and Ethical Approval details.

NSCLC biopsies were obtained from primary tumors or from metastases. Samples were determined as PD-L1 high ($\geq$ 50%) or low (< 50%) using the Roche VENTANA PD-L1 (SP263) assay. Appendix Table A1 (online only) outlines the clinical parameters for the cohort of patients analyzed. All patients were treated with anti–PD-1/PD-L1 therapies (pembrolizumab [n = 103], nivolumab [n = 49], atezolizumab [n = 7], durvalumab [n = 5], and unidentified immunotherapy [n = 24]; Appendix Table A1). Treatment was either monotherapy or in combination with chemotherapy. ICI therapy was given in the first, second, or third line of treatment (Appendix Table A1). For QF-Pro analysis, three consecutive FFPE tissue slices of each patient's sample were provided. One slide was labeled with H&E, and a trained pathologist identified tumoral areas of interest within the sample. The second and third slides were labeled as donor-only and donor-acceptor, respectively (see below).

QF-Pro Assay Principles

QF-Pro (based on the formerly known iFRET in the study by Sánchez-Magraner et al[9]) uses a two-site coincidence labeling assay to detect intercellular PD-1/PD-L1 interactions. Briefly, two primary monoclonal antibodies were used to detect PD-1 and PD-L1, respectively. These antibodies were then labeled with F(ab')$_2$ fragments conjugated to the donor chromophore ATTO488 (for PD-1 detection) and horseradish peroxidase (for PD-L1 detection). Tyramide signal amplification was used to label the F(ab')$_2$-horseradish peroxidase with the acceptor chromophore Alexa-594. The lifetime of the donor in the presence or absence of the acceptor was recorded using 488-nm laser excitation. The reduction of donor lifetime (caused by resonance energy transfer) in the presence of the acceptor reports on distances of 1-10 nm and therefore acts as a chemical ruler, which can quantify receptor-ligand interactions. See the Data Supplement [Appendix I] for details on QF-Pro labeling assay and acquisitions. The procedure allows the quantification by FRET of protein–protein interaction as was described in the studies by Sánchez-Magraner et al.[9,10]

Statistical Analysis

Data were tested for normality using the Shapiro-Wilks test, resulting in sufficient evidence of non-normality. Box-and-whisker plots were generated using GraphPad Prism 9 (GraphPad, San Diego, CA). Here, the boxes represent the 25%-75% range of the data and the whiskers represent the minimum and maximum values. GraphPad Prism 9 was also used to calculate Cox regression for survival analysis to assess which factors (age, sex, tumor stage, and interaction state) were affecting OS (Table 1). Patients with NSCLC were ranked in order of their mean FRET efficiencies (interaction status) and split into two groups, those with the lowest 60% of average FRET efficiencies and those with the highest 40%. The webtool, Cutoff Finder, was used to objectively define a cutoff point for survival analysis. The tool, described by Budczies et al,[11] uses R scripts.[11] Within the webtool, log-rank survival significance was used and determined the cutoff point in groups to be the lowest 60% and highest 40% of FRET efficiencies. The log-rank (Mantel–Cox) test was performed to determine significant differences between the groups. Kaplan-Meier curves were then plotted using GraphPad Prism 9 and Spearman's r (r_s) coefficient calculated.

TABLE 1. Cox Regression Table Showing That the Only Variable Predicting OS With Statistical Significance Is PD-1/PD-L1 Interaction State as Determined by QF-Pro (HR, 0.8066; 95% CI, 0.6992 to 0.9153; P = .018).

Parameter	HR	95% CI	IZI	P	Significance
PD-1/PD-L1 interaction state	0.8066	0.6992 to 0.9153	3.128	.0018	**
PD-L1 expression	0.9933	0.9839 to 1.002	1.424	.1544	n.s.
Sex	1.224	0.7458 to 1.997	0.8095	.4182	n.s.
Age at diagnosis	1.012	0.9845 to 1.042	0.8599	.3898	n.s.
Line of treatment [1st]	6.764	0.3267 to 50.03	1.635	.102	n.s.
Line of treatment [2nd]	1.044	0.5451 to 1.980	0.1318	.8951	n.s.
Line of treatment [3rd]	1.062	0.2266 to 3.672	0.08671	.9309	n.s.
Mono- versus combination therapy	0.6655	0.3377 to 1.263	1.212	.2256	n.s.
Biopsy location	0.7651	0.4511 to 1.258	1.029	.3036	n.s.

NOTE. Table shows that the only variable significantly predicting OS is the PD-1/PD-L1 interaction state as determined by QF-Pro (HR, 0.8066; 95% CI, 0.6992 to 0.9153; P = .0018 [**]).

Abbreviations: HR, hazard ratio; n.s., not significant; OS, overall survival; QF-Pro, quantitative functional proteomics.
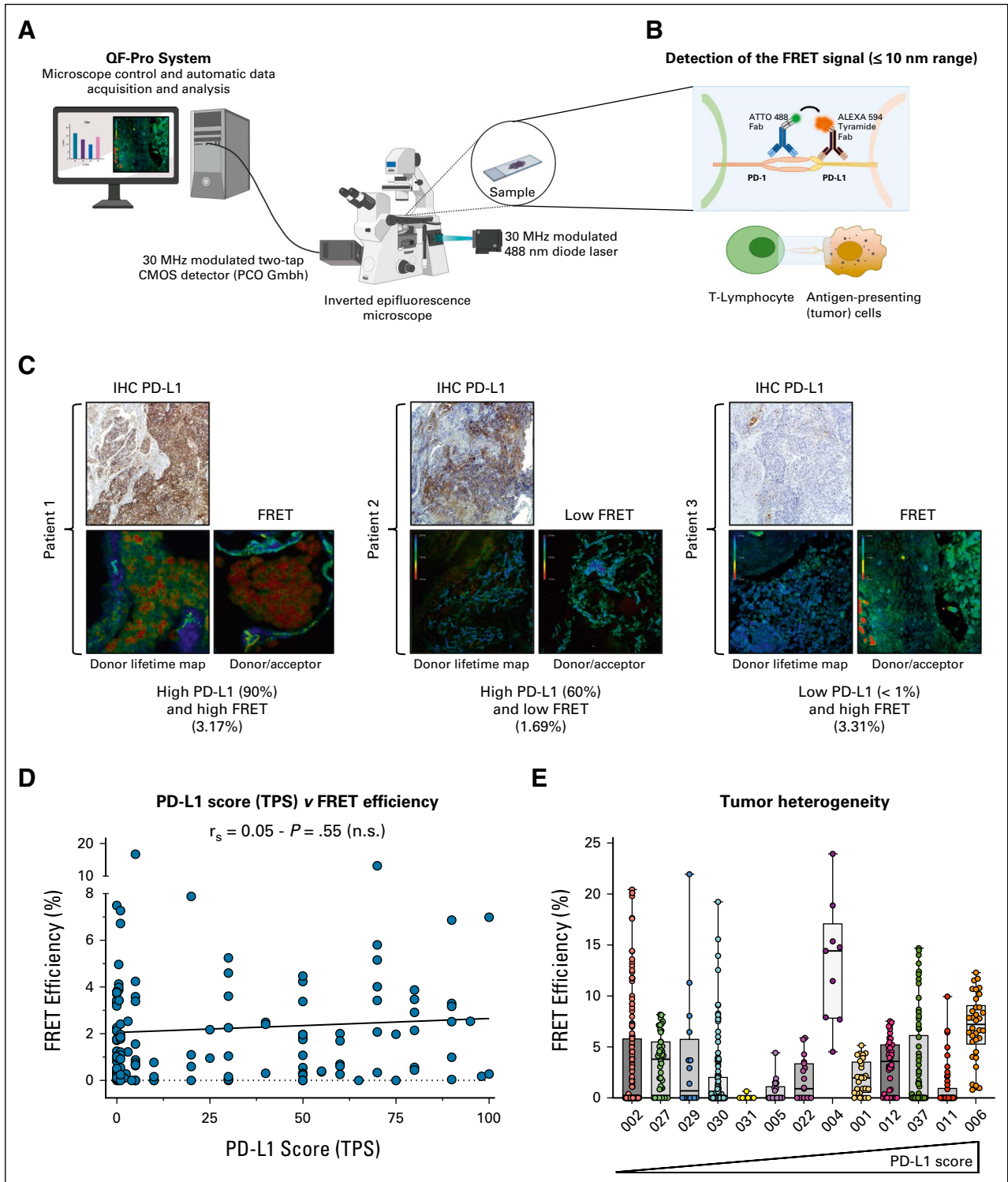
FIG 1. QF-Pro detects a high degree of inter- and intratumoral heterogeneity in PD-1/PDL1 interaction. (A) Schematics of the QF-Pro platform. QF-Pro is a FRET/FLIM platform that is able to quantify PD-1/PD-L1 interactions over a distance of 1-10 nm. It uses an inverted epifluorescence microscope coupled to a 30-MHz modulated diode laser. The detector is a two-tap CMOS detector that is also modulated at 30 MHz in a homodyne manner. (B) Principle of the QF-Pro assay. The assay uses a cell–cell–compatible amplified FRET method, detected by FRET/FLIM. It is a two-site assay that determines the interactive states of the immune checkpoint ligands and receptors engaged between cells. Both the receptor (PD-1) and the ligand (PD-L1) are labeled with a primary antibody of different species. The primary antibodies are then labeled with a F(ab')$_2$ fragment conjugated to ATTO488, for the donor chromophore, and the other with a F(ab')$_2$ fragment conjugated to HRP. Using Tyramide signal amplification, the HRP labels the sample with the acceptor chromophore Alexa594. (C) Clinical PD-L1 images show the (continued on following page)

FIG 1. (Continued). PD-L1 TPS expression, determined by IHC (SP263 Ventana Roche), on three patient samples. Below, the pseudocolored FLIM images are presented. The left panels show the lifetime maps of the FRET donor alone (no interaction). The right panels show the lifetime map of the FRET donor in the presence of the FRET acceptor. A reduction of donor lifetime in the presence of the acceptor (indicated by a change of pseudocolor from blue to green, yellow, and red depending on the FRET efficiency) represents the functional interaction of PD-1/PD-L1 within a patient sample. In these three examples, a discrepancy between FRET efficiency and PD-L1 expression is visible. (D) Correlation plot shows no correlation between PD-L1 scores and FRET efficiency (each blue dot represents a patient's sample—Spearman r = 0.05; P = .55). (E) Mean FRET efficiency measurements within a selection of patient detected a large degree of inter- and intratumoral heterogeneity. Each box plotted here represents one patient, with the dots representing different tumoral areas analyzed per patient. The NSCLC samples analyzed here have a high degree of intratumoral heterogeneity and also interpatient heterogeneity. Patients classified in order of increasing clinical PD-L1 score showed no correlation with PD-1/PD-L1 interaction state. CMOS, Complementary Metal Oxide Semiconductor; FLIM, fluorescence lifetime imaging microscopy; FRET, Förster resonance energy transfer; HRP, horseradish peroxidase; IHC, immunohistochemistry; n.s., not significant; NSCLC, non–small-cell lung carcinoma, QF-Pro, quantitative functional proteomics; TPS, tumor proportion score.

RESULTS

Development of a Novel Quantitative Imaging Platform to Detect PD-1/PD-L1 Functional Interaction in NSCLC Tumor Samples

On the basis of our previously established iFRET assay (Figs 1A and 1B),[9,10] we developed the QF-Pro platform to determine the interaction of the PD-1 receptor with its ligand PD-L1 in FFPE tumor samples (see a more detailed description of the figure in the Data Supplement [Appendices I and II]). The FRET images (Fig 1C) and the box-and-whisker plot demonstrate the large inter- and intratumoral heterogeneity of PD-1/PDL1 interaction in patients' samples (Fig 1E). No correlation can be seen between PD-L1 expression and PD-1/PD-L1 interaction (Fig 1D).

High PD-1/PD-L1 interaction status is predictive of better OS in patients with NSCLC. The OS and PFS (Fig 2) of a cohort of patients with NSCLC (n = 135; Appendix Table A1) were unblinded. Patient samples obtained from hospitals and biobanks from Spain, France, and the Netherlands (see the Materials and Methods section) were analyzed and stratified by FRET efficiency or according to their PD-L1 expression scores (TPSs). It is important to note that all the patients in this cohort were treated with immunotherapy as monotherapy or in combination with chemotherapy. Appendix Table A2 (online only) highlights a more detailed insight into the median of high versus low FRET efficiencies and PD-L1 scores obtained for different clinical subsets of patients (male *v* female, monotherapy *v* combination therapy, and first line *v* second and third line). The OS of each patient was analyzed according to the calculated FRET efficiency (Fig 2A). Comparisons were made between those patients with the highest 40% of FRET efficiencies versus the remaining 60% of patients. This grouping was determined using log-rank survival statistics using the webtool Cutoff Finder (see Materials and Methods section).[11] Strikingly, the Kaplan-Meier survival graph indicates that the patients with a higher FRET efficiency (blue line) had a statistically significant higher OS (P < .0001) with a median survival of 31 months, compared with the remaining patients with a lower FRET efficiency (red line) and a median survival time of only 10 months. Appendix

Figure A1A (online only) shows the significant correlation between OS and FRET efficiency. Moreover, the PFS of each patient (Fig 2B) further validates the power of FRET stratification by showing a significantly higher PFS (P < .0001) in high FRET patients (blue line) compared with the remaining patients with a lower FRET efficiency (red line; median progression of 17 months *v* 7 months). However, when the patients were stratified using the clinical cutoff for first-line immunotherapy treatment high (≥ 50% PD-L1) TPS versus low (< 50% PD-L1) TPS (Fig 2C), the difference in OS was not significant (P = .162) with a median OS of 21 months versus 15 months, respectively. There was also no correlation between OS and TPS (Appendix Fig A1B). Similarly, the analysis in Figure 2D confirmed the lack of significant difference in PFS between the patients stratified by the PD-L1 scores (median of 13 months *v* 10 months without progression). Appendix Figure A2A (online only) presents the stratification by FRET efficiency of 188 patients in total. In addition to the 135 patient data analyzed above, 53 more were included without additional clinical information and lacking PD-L1 scores (PD-L1 data have not been made available from one collaborating hospital). Remarkably, the addition of 53 more patients further strengthened the relationship with an increase in the OS of patients presenting a higher FRET efficiency (P < .0001) with a median survival still undefined after 50 months compared with the remaining patients with a lower FRET efficiency who had a median survival of only 11 months. A significant correlation between the FRET efficiency and the OS (r_s = .338; P < .0001) was shown (Appendix Fig A2B).

The analysis of patients' FRET efficiencies and associated PD-L1 scores confirms the predictive value of FRET efficiency on OS, contrasting with their PD-L1 scores. A matrix graph was created where patient data were plotted as mean FRET efficiency as a function of PD-L1 scores (TPS; Fig 3A). The cutoff for the mean FRET efficiency was 2.127%. This threshold divides the patients into 40% of the population having a higher FRET efficiency versus 60% population of patients with lower FRET efficiencies. The threshold for PD-L1 scores was based on the EMA-approved clinical PD-L1 TPS (≥ 50%) being identified as a
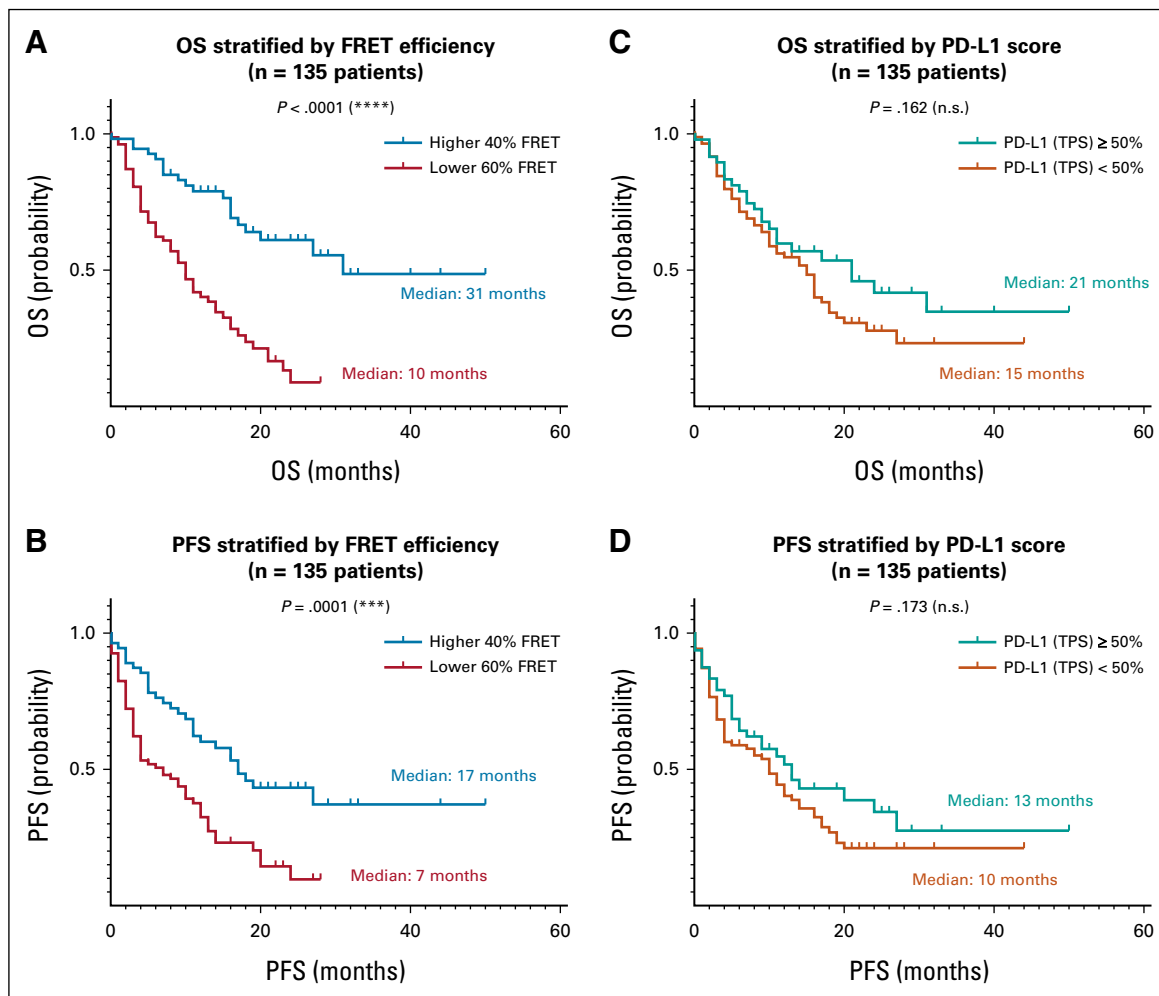
FIG 2. High PD-1/PD-L1 interaction state correlates with a significantly enhanced OS. (A) Patients were analyzed for PD-1/PD-L1 interaction states (mean FRET Efficiency). Patients were stratified into two groups: those with the 40% highest interaction states and those with the lowest 60% interaction states. The 40% population with a higher FRET efficiency (higher interaction state) shows a highly significant improvement of the OS compared with the 60% population with a lower FRET (median 31 v 10 months, $P < .0001$). (B) Patients were analyzed for PD-1/PD-L1 interaction states (mean FRET efficiency). The 40% population with a higher FRET efficiency (higher interaction state) shows a highly significant improvement of PFS compared with the 60% population with a lower FRET (median 17 v 7 months, $P = .0001$). (C) Kaplan-Meier survival curves of patients stratified by their clinical PD-L1 expression. The patients were stratified as PD-L1 high (50% TPS or higher) or PD-L1 low (< 50% TPS). The PD-L1 score stratification is not predictive of a change in overall survival ($P = .162$). (D) Kaplan-Meier survival curves of patients stratified by their clinical PD-L1 expression. The patients were stratified as PD-L1 high (50% TPS or higher) or PD-L1 low (< 50% TPS). The PD-L1 score stratification is not predictive of a change in PFS ($P = .173$). FRET, Förster resonance energy transfer; n.s., not significant; OS, overall survival; PFS, progression-free survival; TPS, tumor proportion score.

high score for first-line immunotherapy. Each quadrant corresponds to patients with a high versus low mean FRET efficiency and a high versus low PD-L1 score. For each of these quadrants, the corresponding Kaplan-Meier curves for OS were determined and a comparison of the survival curves was made between each two quadrants. The top two quadrants showing patients with a high FRET exhibited better OS than the two lower quadrants (low FRET) irrespective of the level of PD-L1 expression (Fig 3B). The patients with low FRET efficiency had a worse OS than the patients with high FRET efficiencies, irrespective of the PD-L1 scores (Fig 3C). Comparison in Figure 3D shows further that high PD-L1 scores are predictive of

better survival only if the associated FRET efficiency is high. Conversely (Fig 3E), patients with low PD-L1 score can, however, show increased OS if they harbor a high FRET efficiency. The graph (Fig 3F) comparing the OS of patients with either a low FRET and high PD-L1 score or a high FRET and low PD-L1 score is a good example of the advantage of determining the state of receptor-ligand engagement directly as a means of predicting the OS. Patients with a high FRET despite harboring a low PD-L1 value had a significantly better OS ($P = .003$) than patients with a low FRET despite the latter's high PD-L1 score. These data clearly demonstrated that having a high PD-L1 score was not predictive of a better OS
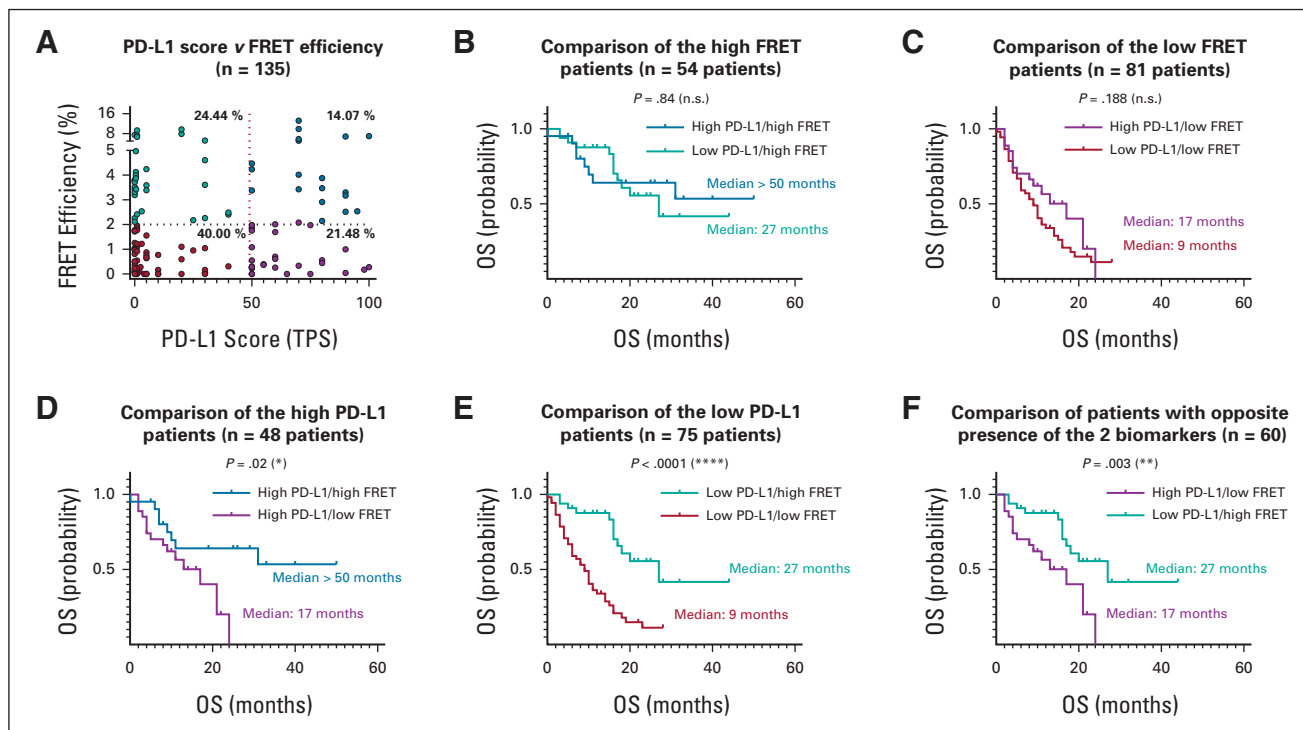
FIG 3. Comparison of the relative influence of PD-L1 expression and PD-1/PD-L1 interaction on OS. (A) The patients' population was categorized according to PD-L1 expression and associated PD-1/PD-L1 interaction states. Patients (each dot represents one patient) were plotted on a matrix on the basis of their mean FRET efficiency (interaction state) and clinical PD-L1 scores and divided into four quadrants. The vertical red line represents the threshold classically applied in clinics for the stratification of patients who should receive or should not receive first-line immunotherapy ($\geq$ 50% PD-L1 score v low < 50% PD-L1, respectively). The horizontal black line represents the 40/60 percent high FRET versus low FRET efficiency cutoff used in our assay stratification. (B-F) Kaplan-Meier analysis comparisons of the patients' OS from each of the matrix categories. (F) shows the very significant difference in OS of patients with a high FRET compared with patients with a low FRET efficiency independent of their PD-L1 expression levels (median OS 27 months versus 17 months; P = .003), indicating that the response to treatment does not depend on PD-L1 expression score. FRET, Förster resonance energy transfer; n.s., not significant; OS, overall survival; TPS, tumor proportion score.

while having a high FRET efficiency correlated with a higher OS.

High FRET efficiency is predictive of response to first- and second-line ICI treatments whereas PD-L1 score is not. Kaplan-Meier analysis was performed to assess the effect of first-line ICI treatment on OS using PD-L1 score (Fig 4A) or using FRET efficiency on OS (Fig 4B) or PFS (Fig 4C) to stratify the patients. As a control, Appendix Table A2 shows that when comparing different subpopulations of patients, there is no bias regarding the overall population that has low versus high FRET efficiency. The graph in Figure 4A shows that the median OS of 78 patients receiving first-line ICI treatment was not significantly different (P = .965) whether they displayed a high or a low PD-L1 score (median 21 months versus 18 months respectively). However, patients with a high FRET efficiency (Fig 4B) had considerably better survival (highly significant P < .0001) in first-line treatments compared with low FRET patients (median 50% survival still undefined after 50 months for high FRET v 11 months for low FRET patients). Moreover, patients with a high FRET efficiency (Fig 4C) responded significantly better to first-line ICI treatment, with a

higher PFS than low FRET patients (27 months v 9 months of PFS). Figures 4D-4F show a similar comparison but with 52 patients who have received ICI in a second line of treatment. Here, also, we observe that the stratification of patients according to their high FRET status yielded increased survival rates (P = .002) and better response to the second line of treatment. However, the difference in median OS and PFS between high and low FRET patients was not as prominent as in first-line treatments. Interestingly, no statistical difference was seen between different therapeutic regimens when stratifying the patients by PD-1/PD-L1 interaction (see the Data Supplement [Appendix III]).

As observed above, stratification by PD-L1 score was not predictive of response to the ICI regimen (P = .196). Remarkably, the PFS of patients receiving ICI in the second line of treatment also showed a significant increase in the patients' PFS when stratified by high versus low FRET efficiency with an 18-month versus 10-month PFS (Fig 4F). These results confirmed the predictive value of the high FRET efficiency for stratifying patients for the ICI treatment line and notably indicate a benefit in treating patients with receptor-
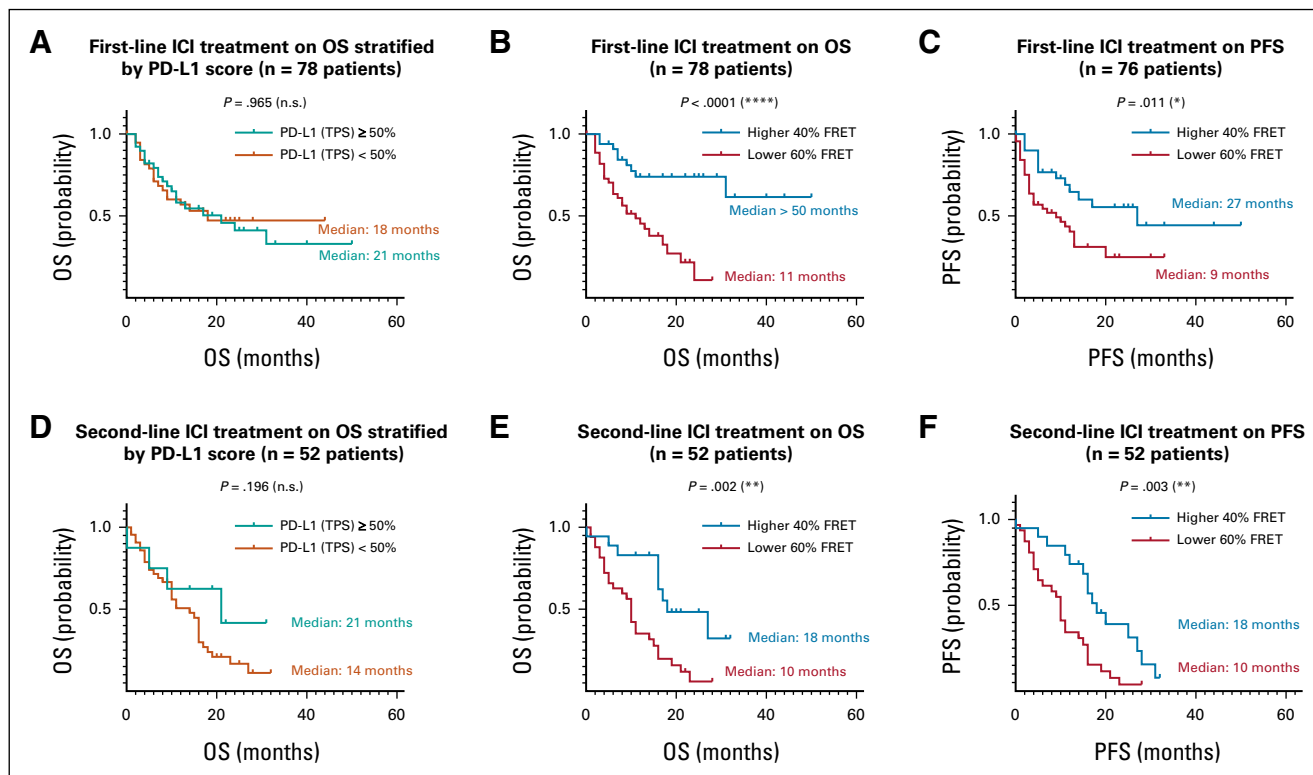
FIG 4. Correlation between FRET efficiency and lines of treatment on OS. (A) Comparison of the OS of patients who have received first-line ICI immunotherapy and stratified by high versus low PD-L1 scores. (B) Comparison of the OS of patients who have received first-line ICI immunotherapy and stratified according to high versus low FRET efficiency (40/60 percent FRET). (C) Patients treated with immunotherapy in first line were analyzed for PD-1/PD-L1 interaction states (mean FRET efficiency). The 40% population with a higher FRET efficiency (higher interaction state) shows a significant improvement of PFS compared with the 60% population with the lowest FRET (median 27 v 9 months, P = .011). (D) Comparison of the OS of patients who have received ICI immunotherapy as second line of treatment either stratified by low versus high PD-L1 scores or (E) stratified by high versus low FRET efficiency. The statistical analysis shows a highly significant prediction on OS using FRET efficiency as a criterion for stratification in first line of treatment (median still undefined at 50 months v 11 months, P < .0001) and in the second line (median 18 v 10 months, P = .002). (F) Patients treated with immunotherapy in the second line were analyzed for PD-1/PD-L1 interaction states (mean FRET efficiency). A higher FRET efficiency (higher interaction state) shows a significant improvement of PFS compared with the 60% population with the lowest FRET (median 18 v 10 months, P = .003). FRET, Förster resonance energy transfer; ICI, immune checkpoint inhibitor; n.s., not significant; OS, overall survival; PFS, progression-free survival.

ligand engagement (high FRET) in first line with ICI treatment rather than deferring to second line. Of note, despite the lack of significance of the PD-L1 stratification on OS in the second line, there is a trend showing a possible benefit of the ICI treatment on OS in patients having a high PD-L1. The impact of treating patients at the earliest opportunity is further presented when comparing metastatic and nonmetastatic patients (see the Data Supplement [Appendix IV]).

DISCUSSION

In this study, we have evaluated the predictive power of measuring PD-1/PD-L1 interaction in situ in comparison with the gold standard of PD-L1 expression level to stratify patients with NSCLC to anti–PD-1/PD-L1 treatment response (refer to the Data Supplement [Appendix V] for a detailed discussion of these results). To do so, we have used a novel bioimaging platform, QF-Pro, for the quantification of PD-1/PD-L1 interaction states in outcome-blinded

FFPE NSCLC samples. The samples were obtained at diagnosis or at surgical resection, and their PD-L1 scores were assessed. Importantly, all patients were subsequently treated with anti–PD-1/PD-L1 therapies. Strikingly, patients with a high PD-1/PD-L1 interaction (determined by QF-Pro) showed a highly significant survival benefit from ICI treatments independent of PD-L1 score. The data demonstrate the power of measuring the PD-1/PD-L1 interaction state in predicting not only patient response to treatment (PFS) but also better OS prediction. Moreover, the lack of correlation between PD-1/PD-L1 interaction states and PD-L1 expression determined by IHC was repeatedly confirmed. High PD-L1 TPS did not predict response to treatment on PFS and only weakly correlated with OS in specific subpopulations. In addition, patients with low PD-L1 scores responded to IO treatment only when they presented a high PD-1/PD-L1 engagement. These data suggest that PD-1/PD-L1 interaction could be used as an additional biomarker

to include the subpopulation of patients with low PD-L1 scores who would benefit from first-line IO treatments.

The stratification of patients receiving immunotherapy in the first or second line using PD-1/PD-L1 engagement clearly revealed that the first-line treatment resulted in a much improved PFS and OS compared with second-line treatment. In addition, we were able to stratify metastatic patients using PD-1/PD-L1 interaction correlating with better OS, although nonmetastatic patients showed better responses. Altogether, these results confirmed the importance of early detection and early use of IO treatments and revealed that, at present, many patients could be missing critical windows of opportunity by not receiving immunotherapy early in their treatment pathway.

Although QF-Pro successfully quantified PD-1/PD-L1 complex formation and demonstrated a clear potential for patient stratification, the study contained limitations. First, PD-L1 scores are more intuitive than FRET efficiency values. Nevertheless, it is the high dynamic range of FRET efficiency that allows for the objective quantification of small changes in complex formation. A consequence of this dynamic range is the generation of data sets, which exhibit large intra- and interpatient heterogeneity. To address this operationally, the analytical process was as follows: Where a pathologist had indicated areas of interest on a pathology slide for QF-Pro analysis, we sought to acquire all ROIs within these regions. If no areas were specifically selected by a pathologist, we analyzed 50 ROIs or the entire tissue, whichever value was greater. This approach mitigated against intrasample heterogeneity. Day-to-day variations may occur analytically, which may present an implementation problem when analyzing patients whose interaction state is at or close to the threshold for treatment (2.127%). It is likely that where implemented, thresholds for treatment decisions are applied conservatively with respect to patients with FRET efficiencies close to this boundary.

The retrospective nature of this study allowed for the correlation of complex formation with OS; however, the authors note that it would be particularly interesting to perform this study in a large prospective cohort allowing for the comparison of patients treated with immunotherapy with patients treated only with chemotherapy, thus assessing the predictive value of this biomarker for IO treatment. To generate an initial view of this question, we assessed the PFS of patients in our cohort who were treated with chemotherapy in first line as a monotherapy regime. The results (Appendix Fig A3, online only) show that there is no difference in PFS between chemotherapy-treated patients stratified by high versus low FRET. This result strongly suggests that the stratification of patients using PD-1/PD-L1 engagement is predictive of the response to IO and is not a general prognostic factor in NSCLC.

A future study would also be required to contain a more comprehensive set of clinical data per patient, with a focus to be put on smoking status as a potential confounder. Finally, although this study indicates that PD-1/PD-L1 engagement is predictive of treatment response and outcome, the technology, as it stands, cannot discern tumor-immune cell interactions from immune-immune cell interactions. It will be of interest to determine the cell types involved and whether this can add value to the stratification observed.

Notwithstanding these limitations, these data provide a compelling case for the functional interrogation of therapeutic targets within patient biopsies. This is exemplified here, where the stratification of patients, through the determination of the extent of PD-1/PD-L1 engagement and not simply ligand expression, is informative for patient stratification and outcome prediction in response to treatments targeting this interaction. Through this approach, patients who are likely to benefit are identified and those not benefitting are able to exploit other distinct interventions. This target status analysis is no doubt germane to a range of biomarker applications for patient stratification and also targeted drug discovery for multiple pathologies.

In summary, the functional data on the extent of PD-L1/PD-1 complex formation offer an objective readout and a cutoff that we show informs on the response to complex disruption. The next step will be to conduct a prospective study that will be critical for the full validation of this IO biomarker.

AFFILIATIONS

[1]HAWK Biosystems (formerly known as FASTBASE Solutions S.L.), Derio, Bizkaia, Spain
[2]Basurto University Hospital, Bizkaia, Spain
[3]Clinica Universidad de Navarra, Idisna, Pamplona, Spain
[4]Cruces University Hospital, Bizkaia, Spain
[5]Galdakao University Hospital, Bizkaia, Spain
[6]Gipuzkoa Cancer Unit, OSID-Onkologikoa, Biodonostia, San Sebastián Spain
[7]Department of pulmonology, Groene Hart Ziekenhuis, Gouda, the Netherlands
[8]Rijnstate Hospital, Arnhem, the Netherlands
[9]Early Phase Trials and Sarcoma, Institut Bergonié, Cours de l'Argonne, Bordeaux, France
[10]University of the Basque Country (UPV/EHU), Leioa, Spain

[11]School of Cancer and Pharmaceutical Sciencess, King's College London, London, United Kingdom
[12]Francis Crick Institute, London, United Kingdom

CORRESPONDING AUTHOR

Véronique Calleja, PhD, HAWK Biosystems (FASTBASE Solutions S.L.)., 612 Astondo Bidea, Science and Technology Park of Bizkaia, Derio, Bizkaia 48160, Spain; e-mail: veronique.calleja@hawkbiosystems.com.

EQUAL CONTRIBUTION

L.S.-M. and J.G. are first coauthors.

DATA SHARING STATEMENT

This was a retrospective study taking place between HAWK Biosystems and various hospitals and biobanks. The clinical samples and data were sent to HAWK Biosystems for processing but belong to the respective hospitals and biobanks. The names of the persons responsible for sending of samples from each hospital/biobank are listed in the supporting Data Sharing Document, online only.

AUTHOR CONTRIBUTIONS

Conception and design: Lissete Sánchez-Magraner, Juan Gumuzio, James Miles, Purificación Martínez del Prado, Fernando Pikabea, Salvador Martín-Algarra, Mónica Saiz-Camin, Mikel Egurrola-Izquierdo, Ander Urruticoechea, Fernando Aguirre, Peter J. Parker, Véronique Calleja
Financial support: Lissete Sánchez-Magraner, Fernando Aguirre, Peter J. Parker, Véronique Calleja
Provision of study materials or patients: Purificación Martínez del Prado, María Teresa Abad-Villar, Fernando Pikabea, Laura Ortega, Carmen Etxezarraga, Salvador Martín-Algarra, María D. Lozano, Mónica Saiz-Camin, Mikel Egurrola-Izquierdo, Inmaculada Barredo-Santamaría, Alberto Saiz-López, Jenifer Gomez-Mediavilla, Nerea Segues-Merino, María Aranzazu Juaristi-Abaunz, Erica J. Geraedts, Kim van Elst, Niels J.M. Claessens, Antoine Italiano
Collection and assembly of data: Lissete Sánchez-Magraner, Juan Gumuzio, James Miles, Nicole Quimi, Purificación Martínez del Prado, María Teresa Abad-Villar, Fernando Pikabea, Laura Ortega, Carmen Etxezarraga, Salvador Martín-Algarra, María D. Lozano, Mónica Saiz-Camin, Mikel Egurrola-Izquierdo, Inmaculada Barredo-Santamaría, Alberto Saiz-López, Jenifer Gomez-Mediavilla, Nerea Segues-Merino, María Aranzazu Juaristi-Abaunz, Erica J. Geraedts, Kim van Elst, Niels J.M. Claessens, Antoine Italiano, Christopher J. Applebee, Sandra del Castillo, Charles Evans, Fernando Aguirre, Peter J. Parker, Véronique Calleja
Data analysis and interpretation: Lissete Sánchez-Magraner, Juan Gumuzio, James Miles, Purificación Martínez del Prado, Fernando Pikabea, Laura Ortega, Carmen Etxezarraga, Salvador Martín-Algarra, Mónica Saiz-Camin, Mikel Egurrola-Izquierdo, Inmaculada Barredo-Santamaría, Alberto Saiz-López, Niels J.M. Claessens, Fernando Aguirre, Peter J. Parker, Véronique Calleja
Manuscript writing: All authors
Final approval of manuscript: All authors
Accountable for all aspects of the work: All authors

REFERENCES

1. Aldarouish M, Wang C: Trends and advances in tumor immunology and lung cancer immunotherapy. J Exp Clin Cancer Res 35:157, 2016

2. Man J, Millican J, Mulvey A, et al: Response rate and survival at key timepoints with PD-1 blockade vs chemotherapy in PD-L1 subgroups: Meta-analysis of metastatic NSCLC trials. JNCI Cancer Spectr 5:pkab012, 2021

3. Qin S, Xu L, Yi M, et al: Novel immune checkpoint targets: Moving beyond PD-1 and CTLA-4. Mol Cancer 18155:155, 2019

4. Gridelli C, Ardizzoni A, Barberis M, et al: Predictive biomarkers of immunotherapy for non-small cell lung cancer: Results from an experts panel meeting of the Italian association of thoracic oncology. Transl Lung Cancer Res 6:373-386, 2017

5. Savic Prince S, Bubendorf L: Predictive potential and need for standardization of PD-L1 immunohistochemistry. Virchows Arch 474:475-484, 2019

6. Niu M, Yi M, Li N, et al: Predictive biomarkers of anti-PD-1/PD-L1 therapy in NSCLC. Exp Hematol Oncol 10:18, 2021

7. Veeriah S, Leboucher P, de Naurois J, et al: High-throughput time-resolved FRET reveals Akt/PKB activation as a poor prognostic marker in breast cancer. Cancer Res 74:4983-4995, 2014

8. Miles J, Applebee CJ, Leboucher P, et al: Time resolved amplified FRET identifies protein kinase B activation state as a marker for poor prognosis in clear cell renal cell carcinoma. BBA Clin 8:97-102, 2017

9. Sánchez-Magraner L, Miles J, Baker CL, et al: High PD-1/PD-L1 checkpoint interaction infers tumor selection and therapeutic sensitivity to anti-PD-1/PD-L1 treatment. Cancer Res 80:4244-4257, 2020

10. Sánchez-Magraner L, de la Fuente M, Evans C, et al: Quantification of PD-1/PD-L1 interaction between membranes from PBMCs and melanoma samples using cell membrane microarray and time-resolved förster resonance energy transfer. Analytica 2:156-170, 2021

11. Budczies J, Klauschen F, Sinn BV, et al: Cutoff finder: A comprehensive and straightforward web application enabling rapid biomarker cutoff optimization. PLoS One 7:e51862, 2012

■ ■ ■

AUTHORS' DISCLOSURES OF POTENTIAL CONFLICTS OF INTEREST

Functional Engagement of the PD-1/PD-L1 Complex But Not PD-L1 Expression Is Highly Predictive of Patient Response to Immunotherapy in Non–Small-Cell Lung Cancer

The following represents disclosure information provided by authors of this manuscript. All relationships are considered compensated unless otherwise noted. Relationships are self-held unless noted. I = Immediate Family Member, Inst = My Institution. Relationships may not relate to the subject matter of this manuscript. For more information about ASCO's conflict of interest policy, please refer to www.asco.org/rwc or ascopubs.org/jco/authors/author-center.

Open Payments is a public database containing information reported by companies about payments made to US-licensed physicians (Open Payments).

Lissete Sánchez-Magraner
Employment: Hawk Biosystems
Speakers' Bureau: Hawk Biosystems (Inst)
Travel, Accommodations, Expenses: Hawk Biosystems (Inst)

Juan Gumuzio
Employment: Hawk Biosystems (Formerly Fastbase Solutions)
Leadership: Hawk Biosystems

James Miles
Employment: HAWK Biosystems
Speakers' Bureau: HAWK Biosystems (Inst)
Travel, Accommodations, Expenses: HAWK Biosystems

Nicole Quimi
Employment: Hawk Biosystems

Purificación Martínez del Prado
Speakers' Bureau: AstraZeneca, Pfizer
Travel, Accommodations, Expenses: Gilead Sciences, Pfizer, Sanofi, Roche, LEO Pharma, AstraZeneca, Lilly

Fernando Aguirre
Employment: HAWK Biosystems
Leadership: HAWK Biosystems
Stock and Other Ownership Interests: HAWK Biosystems
Travel, Accommodations, Expenses: HAWK Biosystems

Salvador Martín-Algarra
Consulting or Advisory Role: MSD Oncology
Speakers' Bureau: Bristol Myers Squibb, MSD Oncology, PharmaMar, Roche, AstraZeneca
Travel, Accommodations, Expenses: Roche, MSD

María D. Lozano
Consulting or Advisory Role: MSD Oncology
Speakers' Bureau: Roche, AstraZeneca, Bristol Myers Squibb/Sanofi, MSD Oncology, PharmaMar
Travel, Accommodations, Expenses: Roche, MSD

Ander Urruticoechea
Consulting or Advisory Role: InProTher, Ellipses Pharma
Travel, Accommodations, Expenses: Roche/Genentech, Pfizer, Gilead Sciences

Niels J.M. Claessens
Consulting or Advisory Role: MSD, Janssen Oncology, Bristol Myers Squibb/Sanofi, AstraZeneca

Antoine Italiano
Honoraria: Bayer, Daiichi Sankyo, Lilly, Epizyme, Novartis, Roche, IPSEN
Consulting or Advisory Role: Roche, Daiichi Sankyo, Immune Design, Epizyme, Bayer, Lilly
Research Funding: Roche, Bayer, AstraZeneca/MedImmune, PharmaMar, MSD Oncology, Merck Serono
Patents, Royalties, Other Intellectual Property: BMS

Sandra del Castillo
Employment: HAWK Biosystems S.A

Charles Evans
Employment: LabCorp

Fernando Pikabea
Honoraria: GlaxoSmithKline, MSD Oncology

Peter J. Parker
Stock and Other Ownership Interests: HAWK Biosystems
Consulting or Advisory Role: Apollo Therapeutics

Véronique Calleja
Employment: Hawk Biosystems
Leadership: Hawk Biosystems
Speakers' Bureau: Hawk Biosystems
Travel, Accommodations, Expenses: Hawk Biosystems

No other potential conflicts of interest were reported.
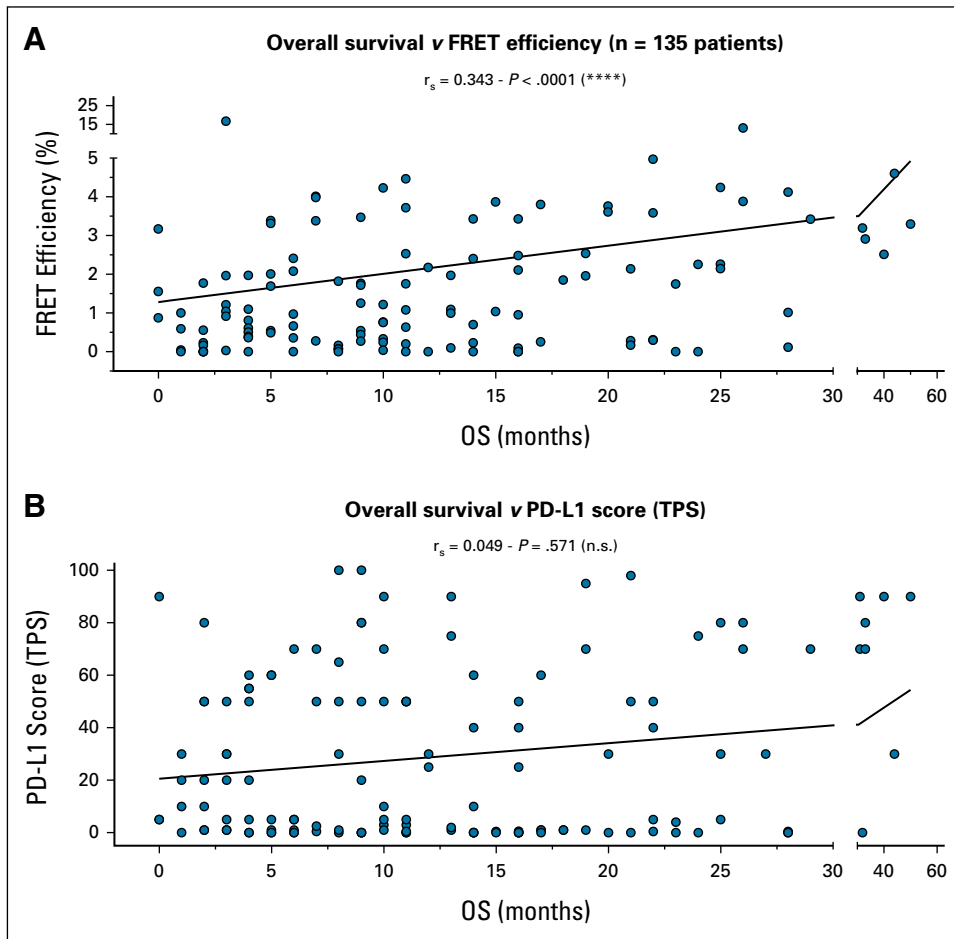
FIG A1. Correlation between OS and FRET efficiency but not with PD-L1 score. (A) The plots from 135 patients show that a highly significant linear correlation exists between the FRET efficiency and the OS (Spearman r = 0.343, $P < .0001$). However, in (B), there is no correlation between OS and PD-L1 scores (Spearman r = 0.049, $P = .571$). FRET, Förster resonance energy transfer; n.s., not significant; OS, overall survival; TPS, tumor proportion score.
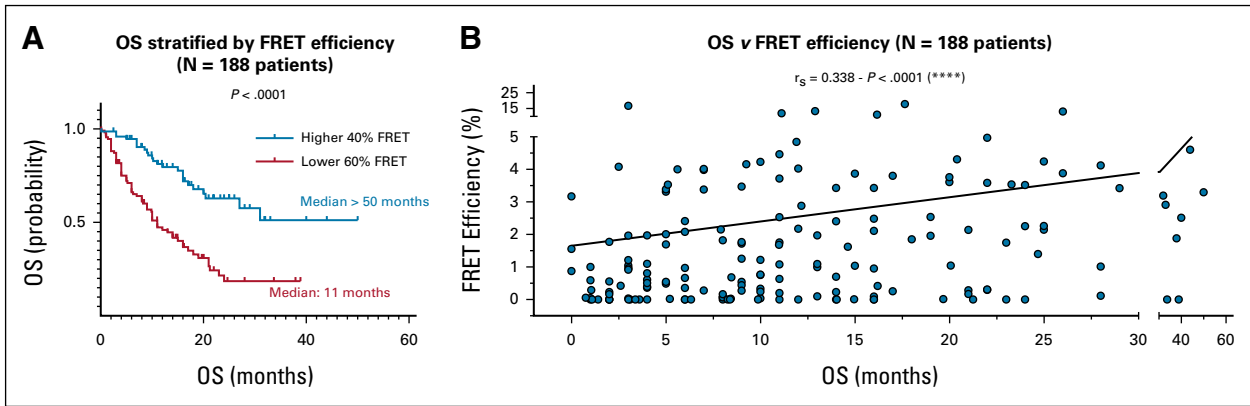
FIG A2. High PD-1/PD-L1 interaction state correlates with a significantly enhanced OS in 188 patients. (A) Patients were analyzed for PD-1/PD-L1 interaction states (mean FRET Efficiency). Patients were stratified into two groups: the 40% highest interaction states population and the lowest 60% interaction states population. The 40% population with a higher FRET efficiency (higher interaction state) shows a highly significant improvement of the OS compared with the 60% population with a lowest FRET (median still undefined at 50 months v 11 months, $P < .0001$). (B) FRET efficiency correlation plot shows a highly significant correlation between FRET efficiency (PD-1/PD-L1 interaction state) and OS (Spearman r = 0.338; $P < .0001$). FRET, Förster resonance energy transfer; OS, overall survival.
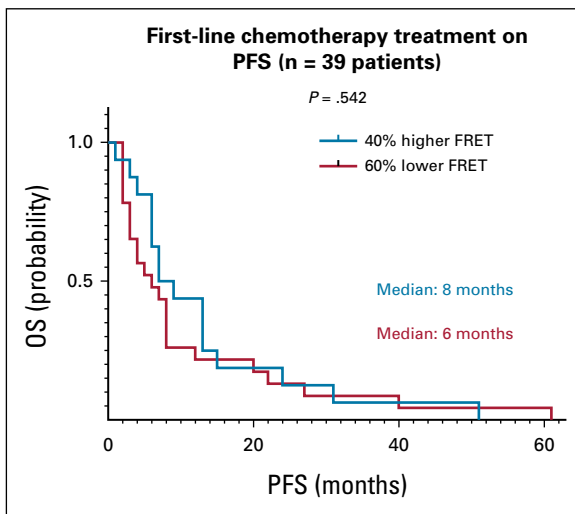

FIG A3. PD-1/PD-L1 engagement is not predictive of response to chemotherapy treatment. Patients who were treated with chemotherapy in first line were analyzed for PD-1/PD-L1 interaction states (mean FRET efficiency). Patients were stratified into two groups: the 40% highest interaction states population and the lowest 60% interaction states population. The 40% population with a higher FRET efficiency (higher interaction state) did not show any significant improvement of PFS compared with the 60% population with a lowest FRET (median 8 v 6 months, $P = .542$). FRET, Förster resonance energy transfer; PFS, progression-free survival.

TABLE A1. Clinical Parameters

Clinical Parameter	Frequency, No. (%)
Sex (n = 135)	
Female	51 (37.8)
Male	84 (62.2)
Age at primary diagnosis, years (n = 134)	
< 50	4 (3.0)
50-59	35 (26.1)
60-69	38 (28.4)
70-79	52 (38.8)
≥ 80	5 (3.7)
Biopsy location (n = 134)	
Primary	92 (68.7)
Metastatic	42 (31.3)
Immunotherapy (n = 135)	
Pembrolizumab	100 (74.1)
Atezolizumab	7 (5.2)
Nivolumab	10 (7.4)
Durvalumab	5 (3.7)
Undefined	13 (9.6)
PD-L1 score (n = 134)	
Negative (< 1%)	34 (25.4)
Low (1%-50%)	66 (49.2)
High (> 50%)	34 (25.4)
Monotherapy (n = 135)	
Yes	86 (63.7)
No	49 (36.3)
Immunotherapy line of treatment (n = 134)	
1st	78 (58.2)
2nd	51 (38.1)
3rd	5 (3.7)

TABLE A2. FRET and PD-L1 Scores Population on Stratification

	Median High FRET Efficiency (%)	Median Low FRET Efficiency (%)	No. of Patients (n = 135)	Median PD-L1 Score	No. of Patients (n = 134)
Monotherapy	3.816	0.442	86	30	85
Combination with chemotherapy	3.695	0.543	49	3	49
First line	3.880	0.394	78	45	78
Second and third line	3.718	0.509	57	2	56
Female	3.987	0.364	51	5	51
Male	3.599	0.648	84	20	83

Abbreviation: FRET, Förster resonance energy transfer.